CrossMark

Vegetation-cloud feedbacks to future vegetation changes in the Arctic regions

Mee-Hyun Cho[1] · Ah-Ryeon Yang[2] · Eun-Hyuk Baek[1] · Sarah M. Kang[3] ·
Su-Jong Jeong[4] · Jin Young Kim[5] · Baek-Min Kim[1]

Abstract This study investigates future changes in the Arctic region and vegetation-cloud feedbacks simulated using the National Center for Atmospheric Research Community Atmosphere Model Version 3 coupled with a mixed layer ocean model. Impacts of future greening of the Arctic region are tested using altered surface boundary conditions for hypothetical vegetation distributions: (1) grasslands poleward of 60°N replaced by boreal forests and (2) both grasslands and shrubs replaced by boreal forests. Surface energy budget analysis reveals that future greening induces a considerable surface warming effect locally and warming is largely driven by an increase in short wave radiation. Both upward and downward shortwave radiation contribute to positive surface warming: upward shortwave radiation decreases mainly due to the decreased surface albedo (a darker surface) and downward shortwave radiation increases due to reduced cloud cover. The contribution of downward shortwave radiation at surface due to cloud cover reduction is larger than the contribution from surface albedo alone. The increased roughness length also transported surface fluxes to upper layer more efficiently and induce more heating and dry lower atmosphere. A relatively smaller increase in water vapor compared to the large increase in low-level air temperature in the simulation reduces relative humidity and results in reduced cloud cover. Therefore, vegetation-cloud feedbacks induced from land cover change significantly amplify Arctic warming. In addition to previously suggested feedback mechanisms, we propose that the vegetation-cloud feedback should be considered as one of major components that will give rise to an additional positive feedback to Arctic amplification.

Keywords Arctic greening · CAM3 · Albedo · Roughness · Vegetation-cloud feedback

1 Introduction

A greater degree and faster rate of warming over the high-latitude terrestrial Arctic region are occurring compared to rising average global temperatures due to various climate feedbacks in the Arctic region (Rothrock et al. 1999; Serreze et al. 2000; ACIA 2005; Chapin et al. 2005; Screen and Simmonds 2010; Pearson et al. 2013). Changes in high-latitude vegetation-ecosystems that cause major feedback processes have been the focus of many studies, with significant efforts to clarify the physical mechanisms of the feedback processes (Chapin et al. 2005; Foley 2005). Considering the various feedback mechanisms over the Arctic region, near future changes in the ecological environment of the terrestrial Arctic are expected to be dramatic (Swann et al. 2010; Miller and Smith 2012; Myers-Smith et al. 2015), as large areas of the Eurasian tundra covering major permafrost regions are exposed to the direct influence of accelerating Arctic warming. Since the year 2000, enhancement of vegetation greenness in the permafrost areas has been

✉ Baek-Min Kim
bmkim@kopri.re.kr

1   Division of Polar Climate Research, Korea Polar Research Institute, Incheon 406-840, Korea

2   Seoul Metropolitical Office of Meteorology, Suwon, Korea

3   School of Urban and Environmental Engineering, UNIST, Ulsan, Korea

4   School of Environmental Science and Engineering, South University of Science and Technology of China, Shenzhen, Korea

5   Green City Technology Institute, Korea Institute of Science and Technology, Seoul, Korea

observed (Tucker et al. 2001; Zhou et al. 2001; Bunn et al. 2007; Bhatt et al. 2010), including expansion of shrubs in Northern Alaska and the pan-Arctic regions (Tape et al. 2006). Jeong et al. (2011a), using an atmospheric circulation model coupled to a dynamic global vegetation model (DGVM) (Levis et al. 2004), showed that grasslands and shrubs in high latitudes are replaced with boreal forests in response to CO_2 doubling, supporting those studies based on observations.

The alteration of the Earth's surface due to forestation or deforestation is regarded as a significant human-induced change. Though on a global scale, radiative forcing estimates of landscape alteration appear to be small (Solomon et al. 2007), in regions where the landscape changes have been intensive, the impact of land use land cover change is comparable to those of greenhouse gases and sea surface temperatures (SSTs) (Pielke et al. 2011; De Noblet-Ducoudré et al. 2012). For example, under global warming, the evaporative cooling effect of tropical forest can mitigate the warming. On the other hand, the low albedo of boreal forests that is induced from decreased snow and increased vegetation enhance the warming (Bonan 2008b). However, though in the high-latitude region, the enhanced greenhouse effect produced from increased water vapor can enhance the warming (Swann et al. 2010).

The albedo effect is prominent among vegetation-climate feedback components over high latitude regions (Levis et al. 1999; Douville et al. 2000; Bonan 2008b). Vegetation changes affect the local climate system by altering the surface energy budget and hydrological cycle (Jeong et al. 2011b). For example, if vegetated surfaces replace permafrost areas, such as snow-covered or barren surfaces, the increased absorption of solar energy due to reduced surface albedo induces additional surface warming (Bonan et al. 1992; Foley et al. 1994; Chapin et al. 2005). In addition, the land surface energy change is the dominant mechanism by which trees directly modify climate at high-latitudes (Swann et al. 2010; Macias-Fauria et al. 2012; Kang et al. 2015). Increases in absorbed shortwave (SW) radiation due to changes in Arctic vegetation are maximized in boreal summer (Chae et al. 2015). The resulting surface and upper-level warming in the high-latitude and Arctic regions caused by vegetation feedback have remote impacts, such as weakening prevailing tropospheric westerly winds (Lawrence et al. 2008; Jeong et al. 2012) and shifting tropical precipitation northward (Swann et al. 2010; Kang et al. 2015).

Although numerous studies of the vegetation-climate feedback over high latitude have emphasized the albedo feedback (Bonan et al. 1992; Foley et al. 1994; Chapin et al. 2005; Levis et al. 1999; Douville et al. 2000; Foley 2005; Bonan 2008a, b; Lawrence et al. 2008; Swann et al. 2010; Jeong et al. 2011a, 2012; Macias-Fauria et al. 2012; Miller

and Smith 2012; Chae et al. 2015), most have focused on changes in upward SW radiation. Surface albedo is the ratio of the upwelling to the downwelling SW radiation at the surface. The upwelling SW radiation at the surface is largely determined by land cover reflectivity. In contrast, downwelling SW radiation at the surface can be altered by clouds, aerosols, and gases. Changes in vegetation type or cover can modify cloud formation through changes in atmospheric circulation (Xue and Shukla 1993; Chapin et al. 2005; Lee et al. 2011; Yamashima et al. 2011).

Numerous studies have identified clouds as a crucial component in amplifying recent Arctic warming (Graversen et al. 2008; Graversen and Wang 2009; Palm et al. 2010; Jun et al. 2016) and future increased greenhouse forcing (Vavrus 2004). Clouds tend to cool the surface by reflecting incoming solar radiation from space while also warming the surface by absorbing and re-emitting longwave radiation from the Earth's surface. In addition, cloud formation is greatly affected by surface conditions, such as snow and sea-ice conditions and vegetation cover (Curry et al. 1996; Vavrus 2004). Even though the abrupt change of vegetation in the permafrost over Arctic region has been reported (Jorgenson et al. 2001; Christensen et al. 2004; Hinzman et al. 2005), there are few studies of vegetation cloud feedbacks. Over mid-latitude regions, higher (lower) frequency convective cloud days have been reported related to high relative density of forest vegetation (crops) on the surface (Carleton et al. 1994). Over the tropical Amazon region, Pinto et al. (2009) investigated Amazonian forest feedbacks on cloud formation.

The objective of this study is to investigate the sensitivity of atmospheric responses to future greening of Arctic tundra and examine the role of vegetation-cloud feedbacks. We investigate atmospheric responses to future changes in the Arctic tundra using a global climate model coupled with a slab ocean model as the ocean component. The simulations adopt surface boundary conditions for different hypothetical plant functional types (PFTs) representing the future Arctic tundra over northern high latitudes. This study is organized as follows. Section 2 discusses the model used in this study and the surface boundary conditions for the simulation. Section 3 describes the direct impacts of vegetation changes and provides descriptions of vegetation-cloud feedbacks induced by surface condition changes. Section 4 provides the summary and discussion.

2 Methods

2.1 Model

We use the National Center for Atmospheric Research (NCAR) Community Atmospheric Model version 3.1

(CAM3.1) atmospheric general circulation model coupled with a slab ocean model (SOM) as the ocean component. The model uses a finite volume dynamical core and a model grid resolution of 2° by 2.5° horizontal resolution with 26 hybrid-sigma levels in the vertical. CAM3.1 is coupled to a uniform depth, motionless, 100 m slab ocean model, which allows the coupled system to have its own SST variability. The SOM represents a uniform (well-mixed) oceanic mixed layer that determines SST by integrating the net surface heat flux. To account for the oceanic heat transfer through the mixed layer bottom, needed to correct model biases, a flux correction (Q-flux) is applied to the SOM. It is constrained with surface fluxes from the last 100 years of a 200-year simulation with CAM3.1, run with prescribed observed climatological SST and sea-ice conditions (Collins et al. 2004). The land-surface processes in CAM3.1 are calculated using Community Land Model version 3 (CLM3) (Oleson et al. 2004) that effectively considers heat, moisture, and momentum fluxes between land surfaces and the atmosphere. The model also considers thermal and hydrological processes at the surface and interior of a near-surface soil layer (Bonan et al. 2002; Oleson et al. 2004; Dickinson et al. 2006).

2.2 Experiments

To investigate the sensitivity of atmospheric responses to future greening of Arctic tundra and examine the role of vegetation-cloud feedbacks, we conduct three 100-year time-slice experiments. The time-slice experiments have the advantage of providing a large statistical sample of the changed climate (Cubasch et al. 1995). The first 20 years are discarded and the remaining 80 years average used to assess the model response to the vegetation cover change in an equilibrium state. The inter-member standard deviation over the high-latitude region is 0.43 K for surface air temperature (SAT), whereas the difference due to the effects of vegetation greening are much larger (seven times) than these inter-member standard deviation values at the 99% confidence level. Other variables analyzed in this study also showed similar high confidence levels.

The control simulation (CONT) is simulated with the climatological PFT representing the present climate (Fig. 1a). Jeong et al. (2011a) showed that northern high latitudes with grass and shrubs will likely be replaced by boreal forests under CO_2 doubling. Hence, in the sensitivity experiments, grass and shrubs poleward of 60°N, which are typical vegetation species found in extreme cold conditions in the tundra, are replaced by boreal forests, which typically occupy the subarctic (boreal) climate. Vegetation cover southward of 60°N is the same as that used in CONT. To examine the model sensitivity to these surface vegetation changes, this study considers different degrees of vegetation cover changes: (1) 'Grass into Boreal Forest' (GtoBF) and (2) 'Grass and Shrub into Boreal Forest' (GStoBF). Each condition corresponds a possible future state of the Arctic tundra with a significant change (GStoBF) and a moderate change (GtoBF) (Fig. 1).
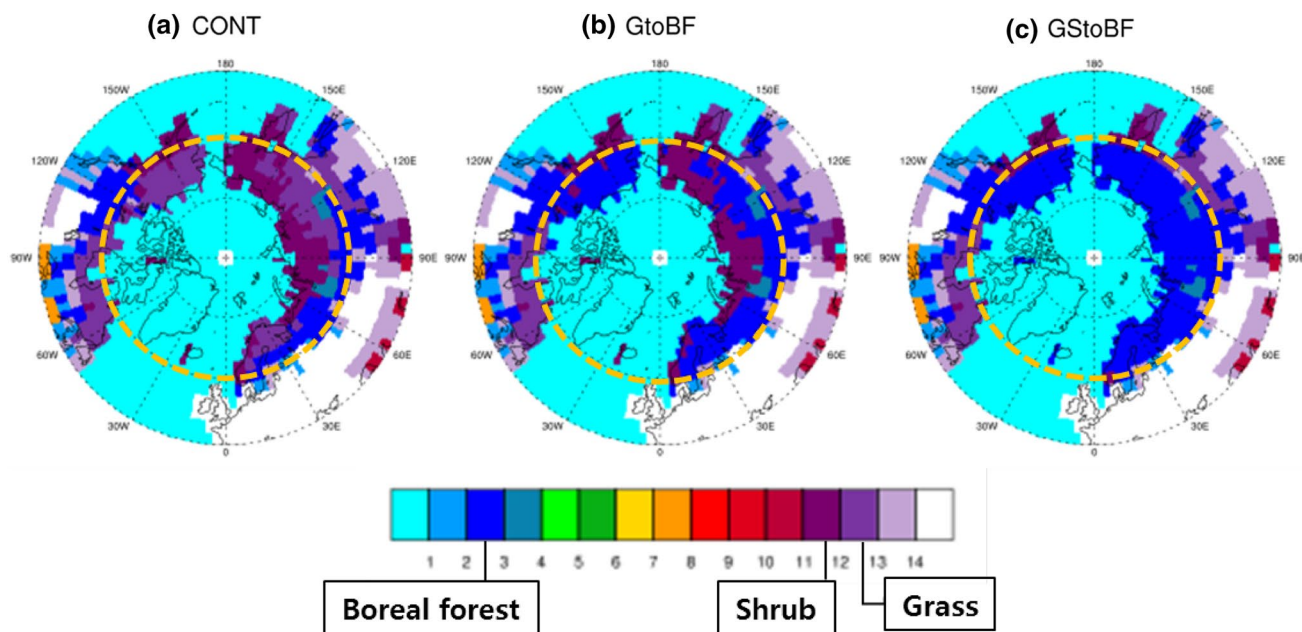

Fig. 1 Arctic vegetation types used for each simulation (CONT: *left*, GtoBF: *middle*, GStoBF: *right*) are represented. Different Plant Functional Types are indicated by *different colors: blue, dark purple and purple* corresponding to boreal forest, shrub, and grass, respectively. The *yellow circle* in each panel indicates the Arctic circle

The model setup is the same as described in Chae et al. (2015) and Kang et al. (2015), except for the use of the finite-volume dynamic core instead of a T42 spectral dynamic core. The atmospheric conditions are prescribed to the 1990s monthly climatology. Except for the surface vegetation distribution, every component, including present-day CO_2 concentrations (335 ppmv), is the same in the three experiments, CONT, GtoBF, and GStoBF. We analyze the differences between the perturbed experiments and the control in the summer growing season (June–August). It must be noted that the bootstrapping methods were performed to determine the significance of differences in means (GtoBF-CONT, GStoBF-CONT) in Figs. 2, 4, and 5. Bootstrapping entails the random resampling of a data set N times, with replacement, to generate N bootstrap samples (Wilks 2006). We obtained 1000 mean differences through this method. The two-sided Student's t test was also performed and the results were very similar to bootstrapping (not shown).

3 Results

3.1 Climate response to changes in high-latitude vegetation cover

To examine the impact of vegetation cover changes, differences in SAT over high-latitudes in GtoBF and GStoBF from CONT are displayed (Fig. 2a, b). Comparing Fig. 2a, b with the vegetation map in Fig. 1, the changes in SAT patterns match the variations in area of vegetation cover. The similarity of spatial warming patterns to surface vegetation cover changes suggests that the increased surface warming is primarily induced by the biophysical effect of local vegetation change. Over the high-latitude Eurasian continent and Alaska, we identified significant increases in SAT, up to about 3 K for GtoBF and 7 K for GStoBF. In Fig. 2, the observed changes are statistically significant at the 99% level in most of regions.

Changes in vegetation type lead to a decrease in surface albedo and an increase in net SW radiation at the surface (Fig. 2c–f). A high-latitude vegetation change over Eurasia and Alaska leads to a major albedo decrease, up to 20%. The regions of large surface albedo change match well with the replaced area of vegetation type, as shown in Fig. 1. Obviously, this is partly due to darker vegetation surfaces reflecting less SW radiation; the boreal forest is much darker than shrubs or grasslands. The change in upward SW radiation at the surface between GStoBF and CONT is 11.5 Wm^{-2}, averaged over 60°N poleward. It is also notable that a significant reduction in albedo and rise in net SW radiation appears in the Arctic Ocean in both cases. This decrease in surface albedo is related to reduced

Arctic sea ice cover, which is most evident over the Laptev, East Siberian, Chukchi, and Beaufort seas (not shown). The darker ocean surface over those regions causes a significant reduction in upwelling SW radiation, which yields a large decrease in surface albedo. In addition, the albedo decrease over the center of the Arctic Ocean is related to snow melt over the sea ice. Therefore, the simulation results indicate that changes in future vegetation cover can induce a sea ice decrease in the Arctic Ocean, further enhancing the positive feedback chain in the Arctic. This result is also consistent with a previous study that investigated the doubling CO_2 response coupled with dynamic vegetation model (Jeong et al. 2014). They state that the increased vegetation brings additional sea ice melting and, therefore, amplifies warming over the Arctic region.

Changes in high-latitude vegetation modify the physical properties of the land surface that affect the surface energy budget. The responses of individual terms in the zonally averaged surface energy budget are shown for GStoBF in the boreal summer (Fig. 3; Table 1). The response in GtoBF differs in magnitude, but is qualitatively similar, therefore, the results from GStoBF will be shown in brevity hereafter. For the latitudinal band 60°N–75°N, where landmass regions show the largest changes in vegetation cover, the dominant response is an increase in net SW radiation (+27.3 Wm^{-2}) at the surface (Table 1). The surface energy balance budget indicates that surface fluxes and longwave radiation compensate for the absorbed SW radiation at the surface. The increased surface temperature from net SW radiation enhances longwave radiation (8.9 Wm^{-2}). Sensible heat fluxes (9.1 Wm^{-2}) toward the lower atmosphere also increase due to the increased surface temperature. In the case of the latent heat flux, biophysical changes from grass and/or shrub to boreal forest further increase the latent heat flux (8.9 Wm^{-2}) through a rise in evapotranspiration. In Fig. 3 and Table 1, the net SW radiation (+27.3 Wm^{-2}), the sum of the downwelling and upwelling SW radiation, is the dominant component and has a positive value. This substantial increase in net SW radiation at the surface is associated with a reduced albedo. The albedo effect is −7%. The upwelling SW radiation change, −7.6 Wm^{-2}, is affected by surface reflectivity. The large decrease in low clouds, −11%, contributes to a considerable increase in downwelling SW radiation, +19.7 Wm^{-2}. The pattern of changes in the downwelling SW radiation (Fig. 4a) matches the variation in area of vegetation cover (Fig. 1). The magnitude of the rise in downwelling SW radiation is much larger than upwelling SW radiation.

Note that the steep increase in net SW radiation 60°N poleward is largely contributed by the increase in downward SW radiation, especially between 60°N–75°N, although both components of SW radiation contribute surplus energy in this latitude band. In contrast, over 75°N poleward, the
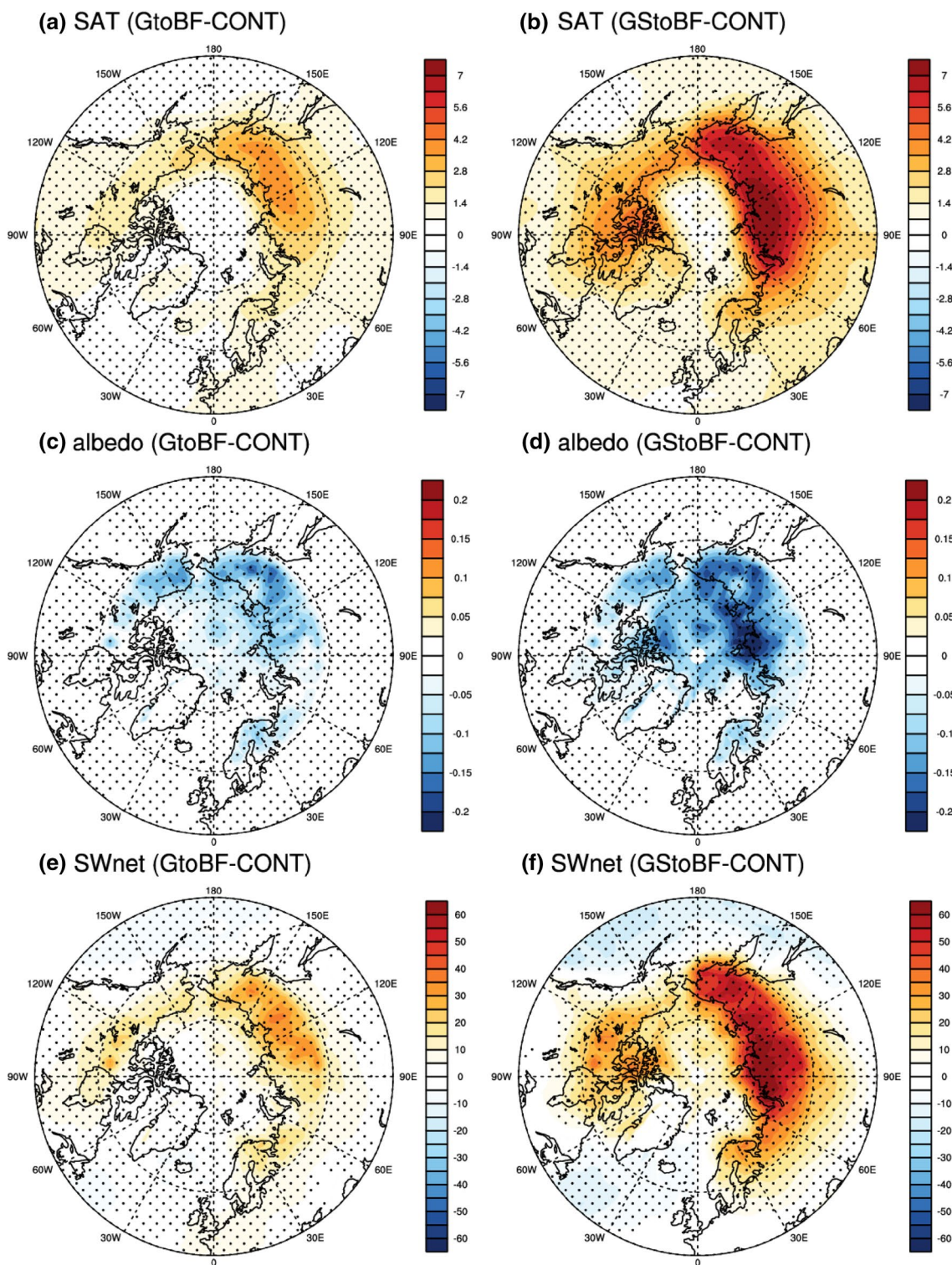
Fig. 2 Surface air temperature (**a, b**); albedo (**c, d**); and net short wave radiation at the surface, Wm^{-2}; **e, f** changes in boreal summer (JJA). **a, c, e** Are for GtoBF minus CONT and **b, d**, and **f** are for GStoBF minus CONT. *Dotted regions* show the confidence lev-els, which indicate that the differences between CONT and GtoBF (CONT and GStoBF) exceeded the 99% bootstrapping significance level
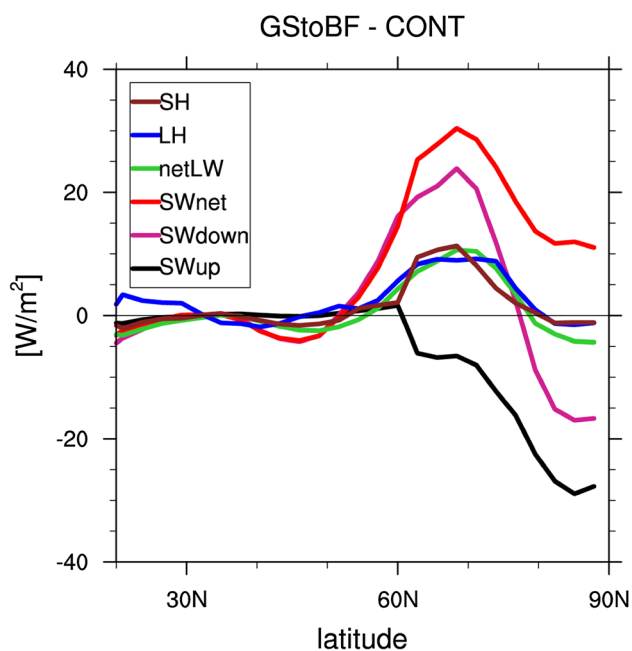
GStoBF - CONT

Fig. 3 Differences in mean summer (JJA) zonal mean surface energy budget (Wm^{-2}). **a** GtoBF minus CONT and **b** GStoBF minus CONT. For the terms of the energy budget, upward shortwave radiation (SWup, *black*), downward shortwave radiation (SWdown, *purple*), net shortwave radiation (SW, *red*), net longwave radiation (LW, *green*), latent heat fluxes (LH, *blue*), and sensible heat fluxes (SH, *brown*) are depicted

Table 1 Changes in the model simulated variables by the land surface changes over high-latitude land (60–75°N)

Variables	Units	GStoBF-CONT
SAT	K	**3.9**
SW down	Wm^{-2}	**19.7**
SW up	Wm^{-2}	**7.6**
SW net	Wm^{-2}	**27.3**
LW net	Wm^{-2}	**8.9**
Latent heat	Wm^{-2}	**8.9**
Sensible heat	Wm^{-2}	**9.1**
Surface albedo	%	**−7**
Low cloud	%	**−11**
PBL height	m	**74.2**

Bold indicates that the difference is statistically significant at a 99% confidence level (bootstrapping)

strong decrease in upward SW radiation induced from additional sea-ice melting leads an increase in net SW radiation. The additional sea-ice melting accounts for the increased vegetation. Because the surface changes from sea-ice to sea surface is much darker than that from shrub/grass to boreal forest, the decrease in solar insolation reflection is much greater over 75°N poleward than southward. However,

the steep increase in downward SW radiation between 60°N–75°N latitude band is unexpected; the source of this steep increase is discussed in Sect. 3.2.

3.2 Vegetation-cloud feedback

As mentioned in Sect. 3.1, the marked warming in Fig. 2 is not solely induced by an increase in absorption of SW radiation due to a decrease in upward SW radiation at the surface. The large increase in downwelling SW radiation, up to 50 Wm^{-2}, also contributed to warming at locations with large changes in vegetation cover (Fig. 4a). The changes in downwelling SW are much larger than changes in upwelling SW radiation (Table 1). Low clouds are highly reflective to solar radiation in the Arctic during summer (Curry et al. 1996; Schweiger and Key 1994; Vavrus and Waliser 2008). The low level cloud cover in GStoBF is reduced by up to 20% over high latitude land with vegetation changes (Fig. 4b). Furthermore, the spatial patterns of downwelling SW radiation at the surface and low cloud fraction are well correlated. SW cloud forcing, defined as the difference between all sky SW radiation and clear sky SW radiation, is positive over that region (Fig. 4c). That is, the region of significant changes in high-latitude vegetation cover experiences increased downwelling SW radiation due to decreased cloud cover. Similar responses appear in GtoBF with smaller magnitudes (not shown). Verification of cloud fraction simulations in polar regions using CAM3 is well documented in Vavrus and Waliser (2008) based on surface observations and several sets of satellite observation data. In comparison, the summer cloud amount simulated by CAM3 fits remarkably well with observations, the error is below 5%.

How do low level clouds decrease in response to surface vegetation changes? Here we propose two possible factors: (1) planetary boundary layer (PBL) height change and (2) low level relative humidity (RH) change. First, the change in surface vegetation can effectively increase PBL height. Two processes, surface albedo change and surface roughness change, can mediate the effects of land surface change through vertical heat transport. As mentioned in Sect. 3.1, over 60°N–75°N, the albedo reduction in GStoBF leads to surface warming, which can produce additional thermal turbulence. The roughness length is also an important factor for mechanical turbulence production that can mix sensible and moisture fluxes from the surface to the atmosphere. The roughness length for vegetation is about 10% of canopy height (Oleson et al. 2004; Bonan 2008a). The canopy height is 14–17 m for boreal forests and 0.5 m for grass and shrubs. Both mechanical turbulence, induced from the roughness change, and thermal turbulence, induced from decreased albedo, enhance mixing of sensible and latent heat fluxes
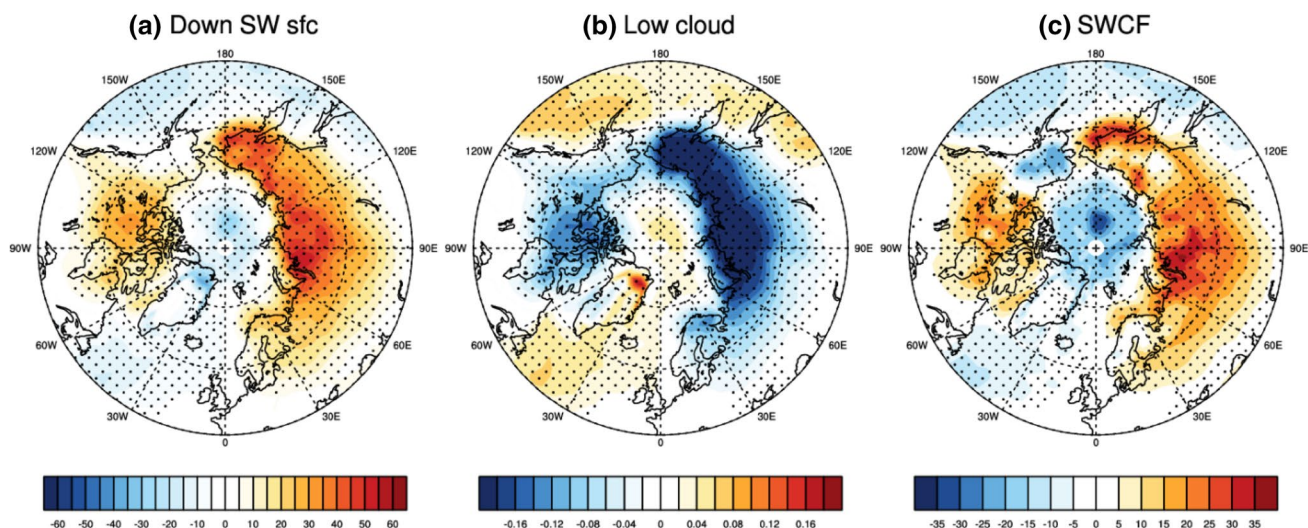
Fig. 4 a Downwelling shortwave flux response at the surface (Wm^{-2}); **b** low cloud fraction; and **c** short wave cloud forcing (Wm^{-2}) for GStoBF minus CONT for boreal summer (JJA). *Dotted regions* show the confidence levels, which indicate that the differences between CONT and GStoBF exceeded the 99% bootstrapping significance level
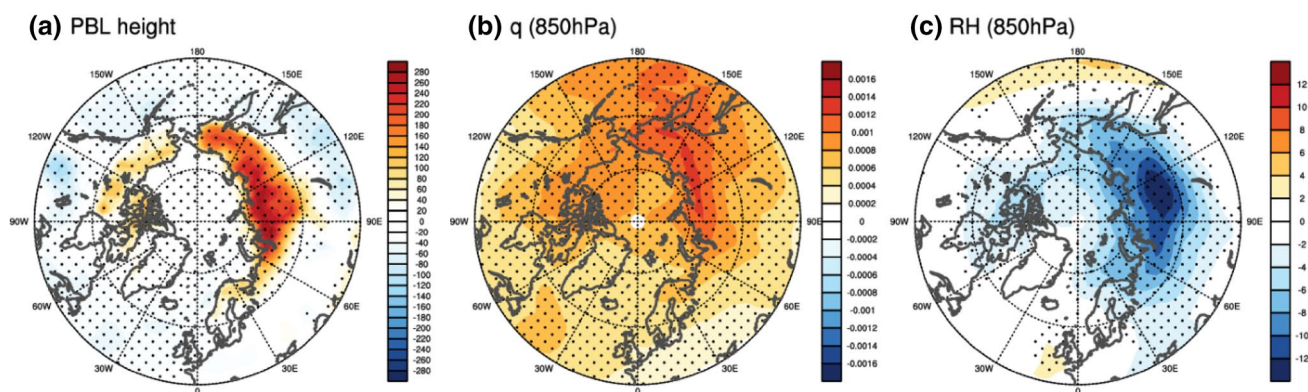

Fig. 5 Changes in **a** PBL height (m); **b** specific humidity (kg/kg, shading) at 850 hPa; and **c** relative humidity at 850 hPa for GStoBF minus CONT for boreal summer (JJA). *Dotted regions* show the confidence levels, which indicate that the differences between CONT and GStoBF exceeded the 99% bootstrapping significance level

to the atmosphere (not shown). The activated vertical mixing extends the boundary layer height and this raises the low cloud bottom height (Fig. 5a).

To examine the relative importance of the surface albedo and roughness, we performed two additional sensitivity experiments based on GStoBF. One is with the albedo of boreal forest unmodified (use the values of grass and shrub as is in CONT), and the other one is with the surface roughness of boreal forest unmodified (use values of grass and shrub as is in CONT). The SAT (RH) difference between each experiment (roughness effect only and albedo effect only) and CONT was similar to 2.3 and 2.6 K (3.6 and 4.4%). This suggests that the effect of roughness length and albedo each contribute significantly to the heating and drying of the lower atmosphere. And their combined effects,

that is, GStoBF, further strengthen warming (3.9 K) and drying (5.1%) of the surface.

Second, surface vegetation change can decrease RH in the lower level. The conversion of Arctic grass and shrub to boreal forest enhances evapotranspiration from vegetation (Goulden et al. 1997, 1998; Bonan 2008b), which leads to an increase in moisture over the high-latitude Eurasian continent and North American continent (Fig. 5b). A black spruce forest in northern Canada lost 2.0–2.5 mm of water per day during the warm summer months (Bonan 2008a). Comparing Fig. 5b with the vegetation map in Fig. 1, the pattern of changes in specific humidity at 850 hPa matches the area of vegetation cover changes. In spite of the increase in specific humidity, RH decreases over the modified vegetation region (Fig. 5c).

To examine the cause for RH reduction, we analyze the vertical structure of temperature and humidity averaged over the regions 60–75°N and 60–150°E, where RH changes are largest (Fig. 6). According to Lawrence (2005), a 5% reduction in RH is accompanied by an increase in the difference between the air temperature (t) and the dew point temperature (t_d) of 1 °C for moist air (RH > 50%).

$$RH \approx 100 - 5(t - t_d) \tag{1}$$

Changes in RH are anti-correlated with changes in $t - t_d$. For example, at 900 hPa, $t - t_d$ increases by 3.5 °C from CONT to GStoBF, and RH is reduced by about 15%. This result implies that the rise in dew point temperature is much smaller relative to air temperature, which leads to a decrease in RH. Environmental RH is an important factor for determining cloud fraction. In global climate models, the threshold RH value is a powerful diagnostic tool for valuating the representation of subgrid variability for cloud fraction parameterizations (Song et al. 2014). Most global climate models, including NCAR CAM3, currently assign the stratus cloud fraction (f) as a function of the gridbox average RH (Vavrus and Waliser 2008):

$$f = \left[\frac{RH - RH_{MIN}}{1 - RH_{MIN}} \right]^2. \tag{2}$$

GStoBF - CONT
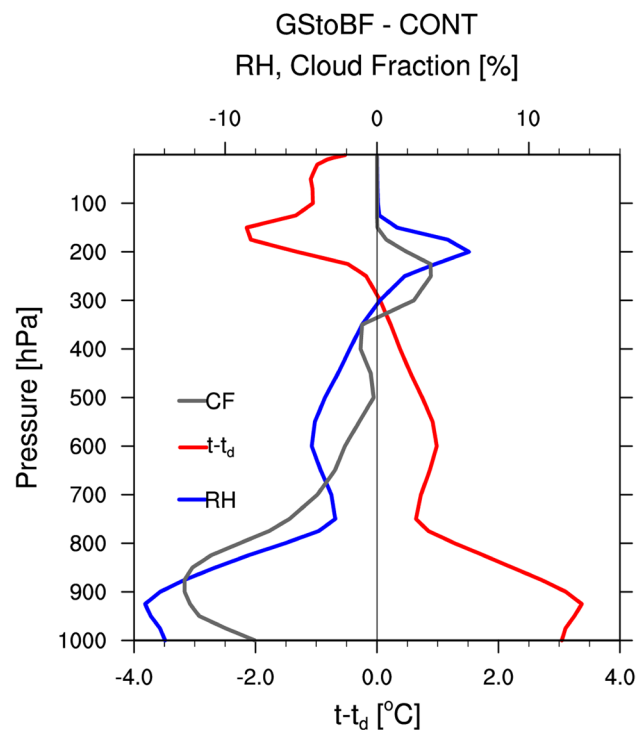RH, Cloud Fraction [%]

Fig. 6 RH (*black*), cloud fraction (*gray*), and difference between temperature and dew point temperature (*red*) profiles averaged over 60–75°N and 60–150°E region for GStoBF minus CONT for boreal summer (JJA)

where RH_{MIN} is the minimum RH at which clouds form (0.8 over land, 0.9 elsewhere). Figure 6 shows that changes in cloud fraction and RH are well correlated. Because GStoBF is forced by surface driven vegetation change, the decrease in cloud fraction is dominant at lower levels (below 700 hPa). The maximized reduction in RH near surface (below 925 hPa) is associated with a PBL height increase, which enhances surface air mixing with relatively dry upper air and induces a decrease in RH in the PBL. The PBL height increase reduces near surface clouds, as mentioned previously. In contrast, the maximum cloud fraction decrease appears near 900 hPa and the difference dwindles along with the reduction in RH difference with height. This implies that surface-driven heating dries the lower troposphere, which enhances a reduction in low-level clouds, as described in Eq. (2). The decrease in low-level clouds causes an increase in downwelling SW, which again leads to surface heating. We call this positive feedback the "vegetation-cloud" feedback.

4 Summary and discussion

We investigated impacts induced by possible future greening of the Arctic region using a slab ocean model coupled to a general circulation model. An increase in net SW radiation due to vegetation cover changes in the Arctic region drives local impacts, most directly by decreasing surface albedo (Fig. 2c, d) and indirectly by decreasing cloud cover over the region (Fig. 4b). The upwelling SW radiation decreases due to reflectivity changes from surface vegetation. Downwelling SW radiation increases considerably following the decrease in clouds as an indirect effect of vegetation change. Consequently, net SW radiation at the surface largely increases. Until now, previous researchers have overlooked this marked increase in downwelling SW radiation at the surface generated by decreasing clouds. This result implies that clouds are a crucial component in the vegetation-climate feedback. The SW input at the surface is balanced by an upward longwave flux, and sensible and latent heat fluxes; this energy balance leads to heating of the lower-level atmosphere. Furthermore, for the first time, a detailed physically plausible explanation for the possible reduction of high-latitude cloud cover is discussed in association with the future vegetation cover changes. Combining with the Intergovernmental Panel on Climate Change (IPCC 2014) report results mainly driven by greenhouse gas forcings, we suggest that the high-latitude cloud cover may not significantly increase by the increase of future greenhouse forcings because of compensating effects of high-latitude vegetation cover described by our study.

As summarized in Fig. 7, the possible future greening of the Arctic region can amplify Arctic warming through
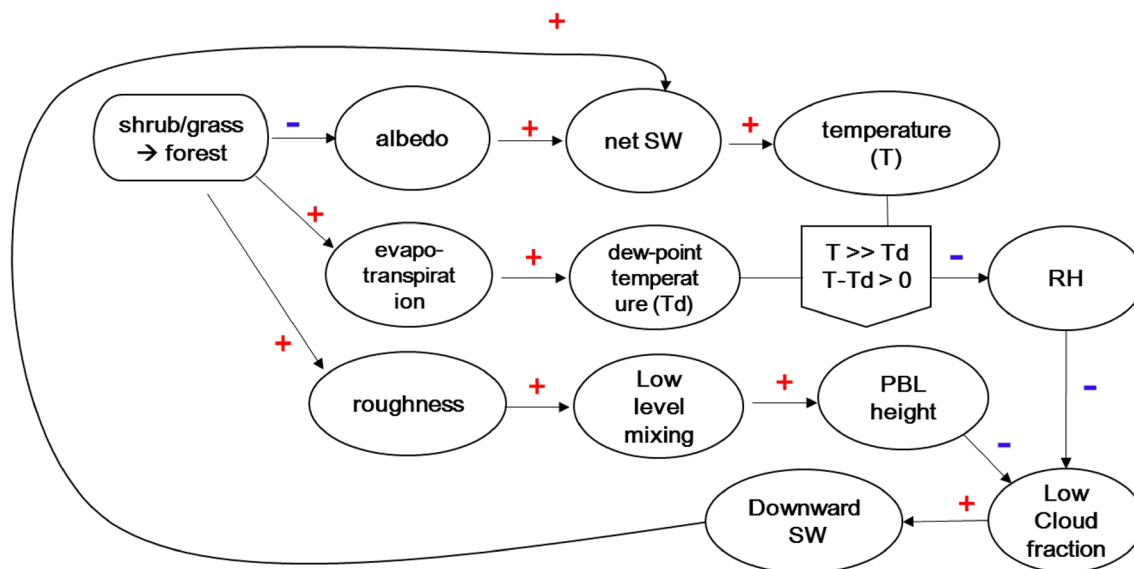
Fig. 7 Vegetation-cloud feedbacks. *Plus* and *minus signs* indicate increasing and decreasing respectively

vegetation-cloud feedbacks. The Arctic land greening induce a reduction in albedo and an increase in roughness length. Both of them contribute to a significant decrease of lower level cloud amount. The increase in PBL height and decreases in low level RH account for the reduction in low level clouds. Smaller increases in water vapor relative to that of air temperature results in an RH reduction. Decreases in cloud fraction account for the increased downward SW radiation. The decrease in low clouds amplifies the SW radiation surplus at the surface and enhances surface heating. We call this positive feedback the "vegetation-cloud" feedback and suggest the feedback be considered as a major component that can give rise to additional positive feedbacks amplifying Arctic warming. Furthermore, this study indicates that the vegetation-cloud feedback may play a role in sea-ice or snow changes.

The amplitude of the response depends on the strength and positioning of local heating. We note that the GStoBF experiment gives us a much stronger heating response, even though the modified vegetation portion is spatially small. The GStoBF experiment modifies the northern coastal terrestrial part of the Arctic region compared with the modification in GtoBF (Fig. 1). This implies that there will be an amplified atmospheric response if the northward tree line migration in the Arctic tundra reaches the northern coastal region.

Although these features are robust and seem to indicate that changes in future vegetation cover in the Arctic will be a major factor modulating future climate, caution is needed in the interpretation. First, this study considered the biogeophysical feedback effect only; the biogeochemical feedback effect was not included. Second, there are large discrepancies in the vegetation distribution between the simulated dynamic vegetation model and the real world. These discrepancies may affect the present results. Third, we used a fixed CO_2 level for the current climate, i.e. 335 ppm, for all simulations, to focus on sensitivity to vegetation cover. Considering the direct warming effect of CO_2 and positive feedback processes over the Arctic region in response to increasing CO_2, our model response may underestimate the magnitude of temperature and circulation response expected in the future. Finally, although the CAM3 simulates cloud amount and related radiation reasonably well during summer, CAM3 has many limitations in macrophysics (Park et al. 2014). We will revisit these feedbacks and results in future work with upgraded version 5, CAM5.

Compliance with ethical standards

Conflict of interest The authors declare that they have no conflict of interest.

References

ACIA (2005) Arctic climate impact assessment. Cambridge University Press, Cambridge

Bhatt US, Walker DA, Raynolds MK, Comiso JC, Epstein HE, Jia G, Gens R, Pinzon JE, Tucker CJ, Tweedie CE, Webber PJ (2010). Circumpolar Arctic tundra vegetation change is linked to sea ice decline. Earth Interact 14(8), 1–20

Bonan GB (2008a) Ecological climatology: concepts and applications. Cambridge University Press, Cambridge

Bonan GB (2008b) Forest and forests and climate change: forcings, feedbacks, and the climate benefits of forests. Science 320(5882):1444–1449

Bonan GB, Pollard D, Thompson SL (1992) Effects of boreal forest vegetation on global climate. Nature 359(6397):716–718

Bonan GB, Levis S, Kergoat L, Oleson KW (2002) Landscapes as patches of plant functional types: an integrating concept for climate and ecosystem models. Glob Biogeochem Cycles 16:1021. doi:10.1029/2000GB001360

Bunn AG, Goetz SJ, Kimball JS, Zhang K (2007) Northern high-latitude ecosystems respond to climate change. EOS 88(34):333–340

Carleton AM, Travis D, Arnold D, Brinegar R, Jelinski DE, Easterling DR (1994) Climatic-scale vegetation—cloud interactions during drought using satellite data. Int J Climatol 14(6):593–623

Chae YJ, Kang SM, Jeong S-J, Kim B-M, Frierson DMW (2015) Arctic greening can cause earlier seasonality of Arctic amplification. Geophys Res Lett. doi:10.1002/2014GL061841

Chapin FS, Sturm M, Serreze MC, McFadden JP, Key JR, Lloyd AH, McGuire AD, Rupp TS, Lynch AH, Schimel JP, Beringer J, Chapman WL, Epstein HE, Euskirchen ES, Hinzman LD, Jia G, Ping CL, Tape KD, Thompson CDC, Walker DA, Welker JM (2005) Role of land-surface changes in Arctic summer warming. Science 310(5748):657–660

Christensen TR, Johansson T, Åkerman HJ, Mastepanov M, Malmer N, Friborg T, Crill P, Svensson BH (2004). Thawing sub-arctic permafrost: effects on vegetation and methane emissions. Geophys Res Lett 31(4):L04501

Collins WD, Rasch PJ, Boville BA (2004) Description of the NCAR community atmosphere model (CAM 3.0). Technical note NCAR/TN-464 + STR. National Center for Atmospheric Research, Boulder

Cubasch U, Waszkewitz J, Hegerl G, Perlwitz J (1995) Regional climate changes as simulated in time-slice experiments. Clim Change 31(2–4):273–304

Curry JA, Rossow WB, Randall D, Schramm JL (1996) Overview of Arctic cloud and radiation characteristics. J Clim 9:1731–1764. doi:10.1175/1520-0442(1996)009<1731:OOACAR>2.0.CO;2

De Noblet-Ducoudré N et al (2012) Determining robust impacts of land-use-induced land cover changes on surface climate over North America and Eurasia: results from the first set of LUCID experiments. J Clim 25:3261–3281. doi:10.1175/JCLI-D-11-00338.1

Dickinson RE, Oleson KW, Bonan GB (2006) The community land model and its climate statistics as a component of the community climate system model. J Clim 19:2302–2324

Douville H, Planton S, Royer JF, Stephenson DB, Tyteca S, Kergoat L, Betts RA (2000) Importance of vegetation feedbacks in doubled-CO_2 climate experiments. J Geophys Res 105(D11):14841–14861

Foley JA (2005) Tipping points in the tundra. Science 310(5748):627–628

Foley JA, Kutzbach JEM, Coe MT, Levis S (1994) Feedbacks between climate and boreal forests during the Holocene Epoch. Nature 371(6492):52–54

Goulden ML, Daube BC, Fan SM, Sutton DJ, Bazzaz A, Munger JW, Wofsy SC (1997) Physiological responses of a black spruce forest to weather. J Geophys Res 102(D24):28987–28996

Goulden ML, Wofsy SC, Harden JW, Trumbore SE, Crill PM, Gower ST, Fries T, Daube BC, Fan SM, Sutton DJ, Bazzaz A, Munger JW (1998) Sensitivity of boreal forest carbon balance to soil thaw. Science 279(5348):214–217

Graversen RG, Wang MH (2009) Polar amplification in a coupled climate model with locked albedo. Clim Dynam 33:629643

Graversen RG, Mauritsen T, Tjernstrom M, Kallen E, Svensson G (2008) Vertical structure of recent Arctic warming. Nature 451:5356

Hinzman LD, Bettez ND, Bolton WR, Chapin FS, Dyurgerov MB, Fastie CL et al (2005) Evidence and implications of recent climate change in northern Alaska and other arctic regions. Clim Change 72(3):251–298

IPCC (2014) Climate change 2014: synthesis report. In: Core Writing Team, Pachauri RK, Meyer LA (eds) Contribution of working groups I, II and III to the fifth assessment report of the intergovernmental panel on climate change. IPCC, Geneva, p 151

Jeong S-J, Ho C-H, Park T-W, Kim J, Levis S (2011a) Impact of vegetation feedback on the temperature and its diurnal range over the Northern Hemisphere during summer in a $2 \times CO_2$ climate. Clim Dyn 37(3–4):821–833. doi:10.1029/2007GL031447

Jeong S-J, Ho C-H, Gim H-J, Brwon ME (2011b) Phenology shifts at start vs. end of growing season in temperate vegetation over the Northern Hemisphere for the period 1982–2008. Global Change Biol 17:2385–2399. doi:10.1111/j.1365-2486.2011.02397.x

Jeong J-H, Kug J-S, Kim B-M, Min S-K, Linderholm HW, Ho C-H, Rayner D, Chen D, Jun S-Y (2012) Greening in the circumpolar high-latitude may amplify warming in the growing season. Clim Dyn 28:1421–1431. doi:10.1007/s00382-011-1142-x

Jeong J-H, Kug J-S, Linderholm HW, Chen D, Kim B-M, Jun S-Y (2014) Intensified Arctic warming under greenhouse warming by vegetation-atmosphere-sea ice interaction. Environ Res Lett 9(9):094007. doi:10.1088/1748-9326/9/9/094007

Jorgenson MT, Racine CH, Walters JC, Osterkamp TE (2001) Permafrost degradation and ecological changes associated with a warming climate in central Alaska. Clim Change 48(4):551–579

Jun S-Y, Ho C-H, Jeong J-H, Choi Y-S, Kim B-M (2016) Recent changes in winter Arctic clouds and their relationships with sea ice and atmospheric conditions. Tellus A 68:29130. doi:10.3402/tellusa.v68.29130

Kang SM, Kim BM, Frierson DM, Jeong SJ, Seo J, Chae Y (2015) Seasonal dependence of the effect of Arctic greening on tropical precipitation. J Clim 28(15):6086–6095

Lawrence, Mark G. (2005) The relationship between relative humidity and the dewpoint temperature in moist air: a simple conversion and applications. Bull Am Meteorol Soc 86(2):225–233. doi:10.1175/BAMS-86-2-225

Lawrence DM, Slater AG, Tinas RA, Holland MM, Deser C (2008) Accelerated Arctic land warming and permafrost degradation during rapid sea ice loss. Geophys Res Lett 35(11):L11506. doi:10.1029/2008GL033985

Lee E, Barford CC, Kucharik CJ, Felzer BS, Foley JA (2011) Role of turbulent heat fluxes over land in the monsoon over East Asia. Int J Geosci 2(04):420

Levis S, Foley JA, Pollard D (1999) Potential high-latitude vegetation feedbacks on CO_2-induced climate change. Geophys Res Lett 26(6):747–750

Levis S, Bonan G, Vertenstein M, Oleson K (2004) The community land model's dynamic global vegetation model (CLM-DGVM): technical description and user's guide. NCAR Tech. Note TN-459 + IA. National Center for Atmospheric Research, Boulder

Macias-Fauria M, Forbes BC, Zetterberg P, Kumpula T (2012) Eurasian Arctic greening reveals teleconnections and the potential for structurally novel ecosystems. Nat Clim Change 2(6):13–18

Miller PA, Smith B (2012) Modelling tundra vegetation response to recent Arctic warming. Ambio 41:281–291. doi:10.1007/s13280-012-0306-1

Myers-Smith IH, Elmendorf SC, Beck PS, Wilmking M, Hallinger M, Blok D et al (2015) Climate sensitivity of shrub growth across the tundra biome. Nat Clim Change 5(9):887–891

Oleson KW, Dai Y, Bonan GB (2004) Technical description of the community land model (CLM). Technical Note NCAR/TN-461 + STR. National Center for Atmospheric Research, Boulder

Palm SP, Strey ST, Spinhirne J, Markus T (2010) Influence of Arctic sea ice extent on polar cloud fraction and vertical structure and implications for regional climate. J Geophys Res-Atmos 115:D21209

Park S, Bretherton CS, Rasch PJ (2014) Integrating cloud processes in the community atmosphere model, version 5. J Clim 27(18):6821–6856

Pearson RG, Phillips SJ, Loranty MM, Beck PS, Damoulas T, Knight SJ, Goetz SJ (2013) Shifts in Arctic vegetation and associated feedbacks under climate change. Nat Clim Change 3(7):673–677

Pielke RA Sr et al (2011) Land use/land cover changes and climate: modeling analysis and observational evidence. WIREs Clim Change 2:828–850. doi:10.1002/wcc.144

Pinto E, Shin Y, Cowling SA, Jones CD (2009) Past, present and future vegetation-cloud feedbacks in the Amazon Basin. Clim Dyn 32(6):741–751

Rothrock DA, Yu Y, Maykut GA (1999) Thinning of the Arctic sea-ice cover. Geo Res Lett 26(23):3469–3472

Schweiger AJ, Key J (1994) Arctic Ocean radiative fluxes and cloud forcing estimated from the ISCCP C2 cloud data set, 1983–1990. J Appl Meteor 33:948–963

Screen JA, Simmonds I (2010) The central role of diminishing sea ice in recent Arctic temperature amplification. Nature 464(7293):1334–1337

Serreze MC, Walsh JE, Chapin FS, Osterkamp T, Dyurgerov M, Romanovsky V, Oechel WC, Morison J, Zhang T, Barry RG (2000) Servational evidence of recent change in the northern high-latitude environment. Clim Change 46(1–2):159–207

Solomon S, Qin D, Manning M, Chen Z, Marquis M, Averyt KB, Tignor M, Miller HL (eds) (2007) Contribution of working group I to the fourth assessment report of the intergovernmental panel on climate change. Cambridge University Press, Cambridge

Song H, Lin W, Lin Y, Wolf AB, Donner LJ, Del Genio AD et al (2014) Evaluation of Cloud Fraction Simulated by Seven SCMs against the ARM Observations at the SGP Site*. J Clim 27(17):6698–6719

Swann AL, Fung IY, Levis S, Bonan G, Doney S (2010) Changes in Arctic vegetation amplify high-latitude warming through the greenhouse effect. Proc Nat Acad Sci 107(4):1295–1300. doi:10.1073/pnas.0913846107

Tape K, Sturm M, Racine C (2006) The evidence for shrub expansion in Northern Alaska and the Pan-Arctic. Glob Change Biol 12(4):686–702

Tucker CJ, Slayback DA, Pinzon JE, Los SO, Myneni RB, Taylor MG (2001) Higher northern latitude normalized difference vegetation index, growing season trends from 1982 to 1999. Int J Biometeorol 45(4):184–190

Vavrus S (2004) The impact of cloud feedbacks on Arctic climate under greenhouse forcing. J Clim 17:603–615

Vavrus S, Waliser D (2008) An improved parameterization for simulating arctic cloud amount in the CCSM3 climate model. J Clim 21:5673–5687. doi:10.1175/2008JCLI2299.1

Wilks DS (2006) Statistical methods in the atmospheric sciences. Academic, San Diego

Xue Y, Shukla J (1993) The influence of land surface properties on Sahel climate. Part I: Desertification. Journal of climate, 6

Yamashima R, Takata K, Matsumoto J, Yasunari T (2011). Numerical study of the impacts of land use/cover changes between 1700 and 1850 on the seasonal hydroclimate in monsoon Asia. J Meteorol Soc Jpn 89 A:291–298 doi:10.2151/jmsj.2011-A19

Zhou L, Tucker CH, Kaufmann RK, Slayback D, Shabanov NV, Myneni RB (2001) Variations in northern vegetation activity inferred from satellite data of vegetation index during 1981 to 1999. J Geophys Res 106(D17):20069–20083